Journal for ImmunoTherapy of Cancer

Mitoribosomal defects aggravate liver cancer via aberrant glycolytic flux and T cell exhaustion

Byong-Sop Song,[1] Ji Sun Moon,[2] Jingwen Tian,[2,3] Ho Yeop Lee,[2,3] Byeong Chang Sim,[2,3] Seok-Hwan Kim,[4] Seul Gi Kang,[3] Jung Tae Kim,[3] Ha Thi Nga,[2,3] Rui Benfeitas,[5] Yeongmin Kim,[6] Sanghee Park,[7] Robert R. Wolfe,[8] Hyuk Soo Eun,[9] Minho Shong,[9] Sunjae Lee,[10] Il-Young Kim,[6,7] Hyon-Seung Yi [1,2,3,9]

To cite: Song B-S, Moon JS, Tian J, *et al*. Mitoribosomal defects aggravate liver cancer via aberrant glycolytic flux and T cell exhaustion. *Journal for ImmunoTherapy of Cancer* 2022;**10**:e004337. doi:10.1136/jitc-2021-004337

► Additional supplemental material is published online only. To view, please visit the journal online (http://dx.doi.org/10.1136/jitc-2021-004337).

B-SS and JSM contributed equally.

Accepted 09 April 2022

For numbered affiliations see end of article.

Correspondence to
Professor Hyon-Seung Yi; jmpbooks@cnu.ac.kr

Dr Il-Young Kim; iykim@gachon.ac.kr

Dr Sunjae Lee; sunjaelee83@gmail.com

ABSTRACT

Background Mitochondria are involved in cancer energy metabolism, although the mechanisms underlying the involvement of mitoribosomal dysfunction in hepatocellular carcinoma (HCC) remain poorly understood. Here, we investigated the effects of mitoribosomal impairment-mediated alterations on the immunometabolic characteristics of liver cancer.

Methods We used a mouse model of HCC, liver tissues from patients with HCC, and datasets from The Cancer Genome Atlas (TCGA) to elucidate the relationship between mitoribosomal proteins (MRPs) and HCC. In a mouse model, we selectively disrupted expression of the mitochondrial ribosomal protein CR6-interacting factor 1 (CRIF1) in hepatocytes to determine the impact of hepatocyte-specific impairment of mitoribosomal function on liver cancer progression. The metabolism and immunophenotype of liver cancer was assessed by glucose flux assays and flow cytometry, respectively.

Results Single-cell RNA-seq analysis of tumor tissue and TCGA HCC transcriptome analysis identified mitochondrial defects associated with high-MRP expression and poor survival outcomes. In the mouse model, hepatocyte-specific disruption of the mitochondrial ribosomal protein CRIF1 revealed the impact of mitoribosomal dysfunction on liver cancer progression. *Crif1* deficiency promoted programmed cell death protein 1 expression by immune cells in the hepatic tumor microenvironment. A [U-$^{13}C_6$]-glucose tracer demonstrated enhanced glucose entry into the tricarboxylic acid cycle and lactate production in mice with mitoribosomal defects during cancer progression. Mice with hepatic mitoribosomal defects also exhibited enhanced progression of liver cancer accompanied by highly exhausted tumor-infiltrating T cells. *Crif1* deficiency induced an environment unfavorable to T cells, leading to exhaustion of T cells via elevation of reactive oxygen species and lactate production.

Conclusions Hepatic mitoribosomal defects promote glucose partitioning toward glycolytic flux and lactate synthesis, leading to T cell exhaustion and cancer progression. Overall, the results suggest a distinct role for mitoribosomes in regulating the immunometabolic microenvironment during HCC progression.

Key messages

What is already known on this topic

⇒ Mitoribosome defects in hepatocellular carcinoma (HCC) are associated with an aggressive phenotype via immunosuppression and immune evasion. However, mechanisms underlying the involvement of mitoribosomal dysfunction in HCC remain poorly understood.

What this study adds

⇒ Mitoribosomal defect alters hepatic glucose metabolism, thereby promoting glucose-derived synthesis of pyruvate and lactate and directing pyruvate toward tricarboxylic acid metabolism. We also found that hepatic mitoribosomal dysfunction induces tumor growth accompanied by highly exhausted tumor-infiltrating T cells in the tumor microenvironment.

How this study might affect research, practice and/or policy

⇒ Immunotherapy targeting the PD-1/PD-L1 checkpoint pathway may show clinical efficacy as a treatment for specific subsets of patients with HCC; efficacy may depend on tumorous expression of mitoribosomal proteins or the level of mitoribosomal dysfunction.

INTRODUCTION

Mitochondria are multifunctional organelles that play critical roles in cellular respiration, biosynthetic metabolism and energy production, generation of reactive oxygen species (ROS) and signaling metabolites, and regulation of cell signaling and apoptosis. Mitochondria are involved in tumorigenesis via mitochondrial stress sensing, which facilitates cellular adaptation to environmental changes.[1] Mitochondria possess their own replication, transcription, and translation machinery, which enables mitochondrial translation using the mammalian mitochondrial ribosome system, also known

as the mitoribosome. The mitoribosome specializes in translation of the 13 mitochondria-encoded membrane proteins, dysfunction of which is associated with human pathologies such as cancer and mitochondrial genetic diseases.[2] Mitoribosomes, macrostructures of dual genetic origin, are formed by three mitoribosomal RNA components encoded by mtDNA and 89 specific mitoribosomal proteins (MRPs) encoded in nuclear DNA.[3] Although mammalian mitoribosomes comprise mostly bacterial ribosomal proteins, mammalian mitoribosomes are distinct from their bacterial and cytoplasmic counterparts in terms of their composition, structure, and mechanistic intricacy.[4] There are mammalian-specific MRPs and early MRPs, the distinct function of which remains to be elucidated, especially with respect to development and progression of cancer.

Owing to the structure, location, and function of the liver, it has many immunological functions, including provision of innate and adaptive immune cells with nutrient-derived antigens and bacterial products.[5] The interaction between antigens and hepatocytes is closely associated with progression of chronic liver disease through activation and regulation of hepatic inflammatory responses.[6] This tolerogenic response to pathogens may promote expansion of tumor-promoting immunoregulatory cell populations, negative regulation of proinflammatory signaling pathways, and development of T cell exhaustion during tumor progression and metastasis. Moreover, the cellular composition of the tumor immune microenvironment is highly complex, with a variety of innate and adaptive immune cell populations playing important roles in inflammation and tumor immune evasion.[7] Despite the central role of the liver in maintenance of immune-metabolic homeostasis, the role of hepatic mitoribosomal dysfunction in regulating liver-resident immune cells is largely undefined in the context of liver cancer development.

CR6-interacting factor 1 (CRIF1), also known as GADD45-associated family protein or mitochondrial ribosomal protein large subunit 59 (MRPL59), is a MRP that plays an essential role in synthesis of mtDNA-encoded oxidative phosphorylation (OxPhos) polypeptides and subsequent insertion of these OxPhos subunits into the inner mitochondrial membrane.[8] Previously, we showed that loss of CRIF1 does not affect ribosome biogenesis; however, qualitative defects or loss of mitoribosome stability disrupt intersubunit assembly. Moreover, CRIF1 interacts with coiled-coil-containing large subunits, which form a structure surrounding the polypeptide exit tunnel.[9 10] In this study, we used a mouse model harboring hepatic mitoribosomal defects to clarify whether *Crif1* deletion-mediated mitoribosomal defects promote progression of liver cancer.

Recently, single-cell profiling has become the avenue of choice to better understand the tumor microenvironment.[11] Mixed populations of tissue-resident and infiltrating cells can be identified and characterized based on their functional status through single-cell profiling in an unbiased way. Here, we characterized the expression profiles of MRPs in patients with hepatocellular carcinoma (HCC), and elucidated the relationship between mitoribosomal defects and cancer prognosis using single-cell and bulk transcriptomics profiling.[12] Interestingly, we observed that malignant cell populations in HCC samples showed mitochondrial dysfunction, and that these defects led to mitochondrial stress, lactate overproduction, and poor survival outcomes (The Cancer Genome Atlas (TCGA) liver cancer cohort). Thus, we also hypothesize that mitoribosomal defect-induced alterations in glucose metabolic flux are associated with liver cancer progression.

METHODS

Human subjects

All experiments were performed in accordance with relevant guidelines and regulations. Written informed consent was obtained from all subjects. Liver tissues were obtained from 50 subjects who underwent hepatectomy at CNUH due to HCC. The baseline characteristics of all subjects are described in online supplemental table S2. Tumor tissue was isolated and used for real-time PCR and flow cytometry analysis.

Mice

To generate liver-specific Crif1 knockout (LivKO) mice, floxed Crif1 (*Crif1$^{f/f}$*) mice were crossed with Albumin-Cre mice (Tg[Alb-Cre]21Mgn), which were purchased from the Jackson Laboratory and had been backcrossed to C57BL/6 J mice. *Crif1$^{f/f}$* mice were used as controls for LivKO mice. All mice were housed in a controlled environment (12 hours light/12 hours dark cycle; humidity: 50%–60%; ambient temperature: 22°C±2°C) in a specific pathogen-free animal facility at the CNUH Preclinical Research Center and fed a normal chow diet. To induce liver cancer, 15-day-old control and LivKO mice received an intraperitoneal injection of 30 mg/kg DEN (Sigma-Aldrich, St. Louis, MO) in 0.9% saline. They were fed a chow diet (Teklad global 18% protein, 2918C, ENVIGO) and used in the experiments at 20 or 40 weeks of age.

Flow cytometry analysis

Hepatic tumorous immune cells were preincubated with anti-mouse CD16/32 Fc blocker (BD Pharmingen, San Diego, CA, USA), followed by staining with the Live/Dead marker FVD-APC-Cy7 (all supplied by eBioscience, San Diego, CA, USA). The fluorochrome-conjugated antibodies used in this study were anti-CD45, anti-CD3, anti-NK1.1, anti-CD4, anti-CD8, anti-CD44, anti-CD62L, anti-CD279, anti-CD11b, anti-F4/80, anti-Ly6C, anti-Ly6C, anti-Siglec-F, anti-MCL-1, and anti-BCL2 (all supplied by eBioscience). Hepatic tumor immune cells were stimulated with phorbol-myristate acetate/ionomycin/brefeldin A/monensin for 5 hours in vitro. Cells were fixed and permeabilized using the Fixation/Permeabilization Buffer kit (eBioscience), washed with FACS

buffer, resuspended in 1% formaldehyde, and stained with anti-IFN-γ-APC. Stained cells were analyzed using a BD LSRFortessa flow cytometer (BD Biosciences, San Jose, CA, USA) and the data were analyzed using the FlowJo software (FlowJo, LLC, Ashland, OR, USA). The antibodies used are listed in online supplemental table S3.

Intraperitoneal injection and constant venous infusion of [U-$^{13}C_6$]-glucose

The oral bolus tracer injection protocol was as follows: mice received [U-$^{13}C_6$]-glucose (50 mg; 25% w/v; 99% enrichment; Cambridge Isotope Laboratories, Cambridge, MA, USA) via oral gavage following a 5-hour fast. After 15 min of [U-$^{13}C_6$]-glucose administration, liver tissue was collected and snap-frozen in liquid nitrogen.

The intravenous infusion protocol was as follows: after a jugular vein catheterization and a subsequent 5-day recovery period, mice received a constant infusion of [U-$^{13}C_6$]-glucose (rate: 20 nmol/g BW/min) via the jugular vein catheter for 150 min. Blood samples were collected 60 min before infusion (to measure background tracer enrichment), and then at 130, 140, and 150 min after initiation of tracer infusion (to measure plateau tracer enrichment). At the completion of infusion, the liver was harvested and snap-frozen in liquid nitrogen.

Other details and additional experimental procedures are provided in online supplemental methods.

RESULTS

MRP expression is associated with mitochondrial stress in malignant cells and poor survival of HCC patients

To identify mitochondrial dysfunction within the tumor microenvironment of HCC, we first checked MRP expression in HCC samples by performing single-cell transcriptome analysis.[13] The data revealed six distinct cell types (figure 1A), namely, malignant cells, cancer-associated fibroblasts, tumor-associated macrophages (TAMs), tumor endothelial cells, B cells, and T cells, along with high expression of MRPs by malignant cells (figure 1B,C; online supplemental figures S1–5).

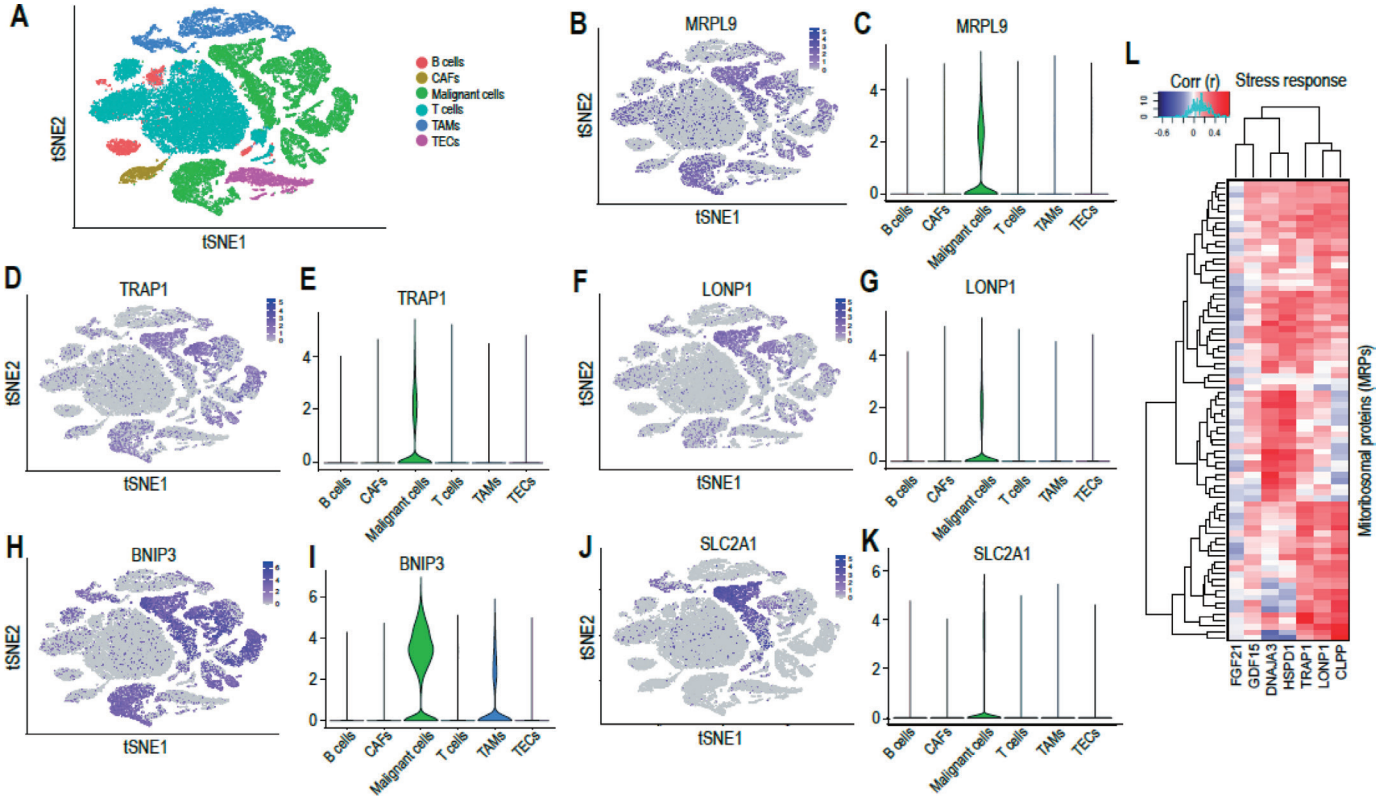

Figure 1 Single-cell transcriptome analysis of HCC samples. Approximately 56,721 single cells from 46 liver tumor samples were analyzed to better understand the tumor microenvironment. (A) t-SNE plot showing identification of various cell types such as B cells, cancer-associated fibroblasts (CAFs), malignant cells, T cells, tumor-associated macrophages (TAMs), and tumor endothelial cells (TECs). (B) tSNE and (C) violin plots showing mitoribosomal protein, MRPL9 expression along with gene expression of mitochondrial stress response proteins, TRAP1 and LONP1, and hypoxia markers BNIP3 and SLC3A1 in various cell clusters. (D) tSNE and (E) violin plots showing TRAP1 expression. (F) tSNE and (G) violin plots showing LONP1 expression. (H) tSNE and (I) violin plots showing BNIP3 expression. (J) tSNE and (K) violin plots showing SLC3A1 expression. (L) TCGA dataset analysis showing coexpression of mitoribosomal proteins (rows) and mitochondrial stress response proteins (columns) across HCC samples. HCC, hepatocellular carcinoma; TCGA, The Cancer Genome Atlas; tSNE, t-Distributed Stochastic Neighbor Embedding.

Next, we explored the gene expression landscape in the six cell types to better understand the tumor microenvironment (figure 1D–K) and identified high expression of *LDHA* in malignant cells and two subsets of T cells (online supplemental figure 6A,B), suggesting a Warburg effect. Interestingly, we also detected elevated expression of genes related to the mitochondrial stress response (eg, *TRAP1* and *LONP1*) and hypoxia (eg, *BNIP3* and *SLC2A1*) in malignant cells, implying mitochondrial defects due to oxygen depletion. Indeed, exposure of HepG2 cells to hypoxia led to upregulation of genes related to mitochondrial stress responses (online supplemental figure 7).

Trajectory analysis revealed that malignant cells and macrophages showed increasing expression of both MRPs and mitochondrial stress-related genes (online supplemental figures S8A–D and S9A–D). Interestingly, we also found that malignant cells showing higher expression of MRP also showed co-expression of mitochondrial stress-related genes and T cell exhaustion markers (online supplemental figure S10A–C). Therefore, we are tempted to speculate that increasing expression of MRPs in the HCC tumor microenvironment is associated with stress responses and subsequent T cell exhaustion.

To further elucidate mitochondrial dysfunction in HCC patients, we analyzed transcriptomic data from a TCGA HCC cohort (N=424). We found that higher expression of MRP in HCC samples correlated positively with expression of mitochondrial stress response proteins (figure 1L). In addition, we observed lower expression of mitochondrial OxPhos subunits in tumor tissues from patients with HCC than in normal livers (online supplemental figure S11A). Moreover, blue native polyacrylamide gel electrophoresis (BN-PAGE) showed a reduction in assembly of OxPhos complexes in mitochondria isolated from tumors compared with non-tumor tissues (online supplemental figure S11B). Conversely, expression of genes related to mitochondrial stress responses also increased significantly in tumor tissues (online supplemental figure S11C). In addition, we identified that higher expression of MRP and mitochondrial stress response proteins was associated significantly with poor survival (log-rank test, $p<0.05$; online supplemental figure S12). Therefore, enhanced expression of MRP during stress responses might be an indicator of mitochondrial defects and a worse prognosis for HCC patients.

Mitoribosomal dysfunction-mediated activation of the mitochondrial unfolded protein response exacerbates progression of DEN-induced liver cancer

To further explore the link between mitochondrial defects and HCC progression, we utilized a mouse model harboring MRP defects. *Crif1*, also named *Mrpl59*, is strongly associated with lower survival rates for HCC patients.[14] Therefore, we selectively disrupted *Crif1* in hepatocytes using the *Cre-loxP* system (online supplemental figure S13A) to determine the impact of hepatocyte-specific impairment of mitoribosomal function on liver cancer progression. CRIF1 expression was significantly lower in liver tissue from liver-specific *Crif1* knockout (LivKO) mice (figure 2A). In line with this, expression of mitochondrial OxPhos complex subunits complex III (UQCRC2) and IV (COX4) was lower in the livers of LivKO mice than in those of control mice (figure 2B; online supplemental figure S13B). Moreover, BN-PAGE analysis revealed a marked reduction in assembly of complex I, III, and V in the livers of LivKO mice compared with those of controls (figure 2C). In addition, the maximal respiration rate and oxygen consumption rate (OCR) were significantly lower in cultured hepatocytes derived from LivKO mice (online supplemental figure S13C); however, the extracellular acidification rate (ECAR) was higher in hepatocytes from LivKO mice than in those from controls (online supplemental figure S13D). Gamitrinib, a mitochondria-targeted HSP90 inhibitor, decreased the basal translation rate; similarly, *Crif1* deficiency attenuated global translation, which may indicate an integrated stress response in the hepatocytes of LivKO mice (figure 2D). In addition, we detected reduced translation ability in both mitochondria and cytosol isolated from the hepatocytes of LivKO mice (online supplemental figure S13E). This suggests that *Crif1* deficiency triggers an integrated stress response, which limits total protein synthesis. Moreover, we found that expression of genes related to the mitochondrial stress response was significantly higher in the livers of LivKO mice than in those of control mice (figure 2E). *Crif1* deficiency-induced mitoribosomal defects significantly increased expression of genes related to mitochondrial stress response in tumor-free mice at 10, 20, and 40 weeks of age (online supplemental figure S13F,G); however, there was no significant difference in tumor expression of OPA and Parkin (online supplemental figure S13H). Although there was no marked difference in the observed hepatic mitochondrial mass on confocal microscopy images from controls and LivKO mice, electron microscopy showed mitochondrial swelling and reduced numbers of cristae in the livers of LivKO mice (online supplemental figure S14A,B).

Next, we investigated alterations in biological processes in the liver tissues of LivKO mice by generating a transcriptome with deep sequencing coverage. Differential gene expression analysis (negative binomial tests, DESeq2 R package) identified 242 significantly upregulated genes, including *Aldoa,* encoding a key enzyme of glycolysis, and 340 downregulated genes, including *Elovl3*, encoding a key enzyme of long chain fatty acid synthesis. We then performed pathway gene set enrichment analysis to compare altered biological processes between LivKO and control mice (figure 2F). We observed that alterations in hepatic metabolism, including upregulation of glycolysis, the tricarboxylic acid (TCA) cycle, and serine metabolism were associated with cancer progression. To better characterize metabolic alterations, we performed reporter metabolite analysis of LivKO mice using a high-quality genome-scale metabolic model (figure 2G,H).[15 16] Interestingly, we observed significant upregulation of most

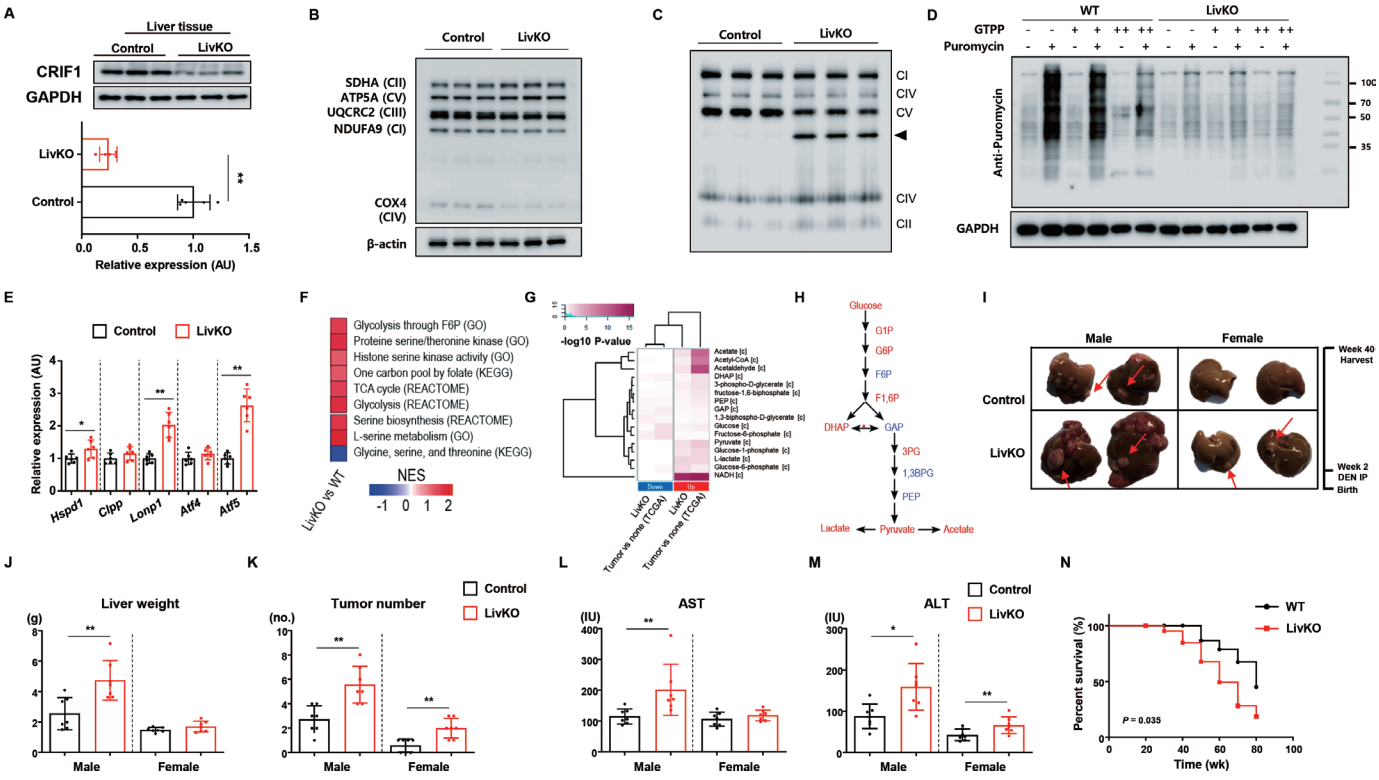

Figure 2 Mitoribosomal defects in hepatocytes promote progression of DEN-induced liver cancer in mice. Liver tissues were harvested from control and LivKO mice at 10 weeks of age and compared. (A) Immunoblotting and qRT-PCR data showing expression of CRIF1. (B) Representative western blot showing expression of OxPhos complex subunits, and (C) representative data from BN-PAGE analysis showing the assembled OxPhos complex. (D) Primary hepatocytes from 8-week-old control and LivKO mice were treated with or without gamitrinib (a mitochondrial matrix chaperone inhibitor) at 1 or 2 µM, followed by treatment with puromycin (1 µg/mL) for 30 min. Cells were harvested for protein extraction and analysis by western blotting using an anti-puromycin antibody to detect basal levels of global translation. (E) qRT-PCR analysis data showing expression of genes related to mitochondrial stress in liver tissues of tumor-free control and LivKO mice. Liver tissues were harvested from control and LivKO mice at 10 weeks of age and compared. (F) Results of pathway enrichment analysis comparing tumor-free control and LivKO mouse transcriptome data (colors correlate with normalized enrichment scores). (G) Comparison of reporter metabolite analysis between TCGA human HCC data and LivKO mouse tumor data. The statistical significance (-log 10 p values) of upregulated metabolites (two rightmost columns) and downregulated metabolites (two leftmost columns) is shown. (H) Visualization of upregulated (red texts) or downregulated (blue texts) glycolysis pathways, as determined by reporter metabolite analysis. Comparative analyses of DEN-treated control and LivKO mice at 40 weeks of age. (I) Representative pictures of liver weight and number of tumor nodules (J, K); and serum levels of alanine aminotransferase and aspartate aminotransferase (L, M). (N) Survival of DEN-treated control and LivKO mice. Data are expressed as the mean±SEM *p<0.05, **p<0.01 ((A, E, J–M): two-tailed t-test; (N): Gehan-Breslow-Wilcoxon test). BN-PAGE, blue native polyacrylamide gel electrophoresis; HCC, hepatocellular carcinoma; qRT-PCR, quantitative reverse transcription-PCR; TCGA, The Cancer Genome Atlas.

glycolytic metabolites, including G6P, lactate, and pyruvate, in the cytosol, thereby reaffirming higher glycolytic flux in LivKO mice than in control mice. Notably, an end-product of glycolysis, lactate, was also enriched in tumor samples from LivKO mice, thereby affecting the tumor microenvironment. In addition, we performed the same reporter metabolite analysis using the TCGA HCC dataset and found similar upregulation of glycolytic process in tumors compared with matched controls, confirming similar trends in both the human and mouse data (figure 2G).

Despite mitochondrial damage and stress being associated with development of tissue damage, tumor invasion, and metastasis,[17 18] LivKO mice did not spontaneously develop liver tumors or abnormal hepatic architecture by 40 weeks of age. We also found no difference in the percentages of exhausted T cells in the livers of controls and LivKO mice (online supplemental figure S14C,D). Although mitoribosomal dysfunction alone did not induce liver cancer in mice, analysis of TCGA datasets revealed an association between the mitoribosome gene set and HCC progression (online supplemental figure S15A–C), along with an association between *CRIF1* mutations and hepatic tumor tissue proliferation (online supplemental table S1). Therefore, we investigated DEN-induced carcinogenesis in the liver of LivKO and control mice. DEN was injected intraperitoneally into 2-week-old weaning mice. When sacrificed at 20 and 40 weeks of age, DEN-treated LivKO mice exhibited rapid progression to aggressive HCC, regardless of gender (figure 2I–K;

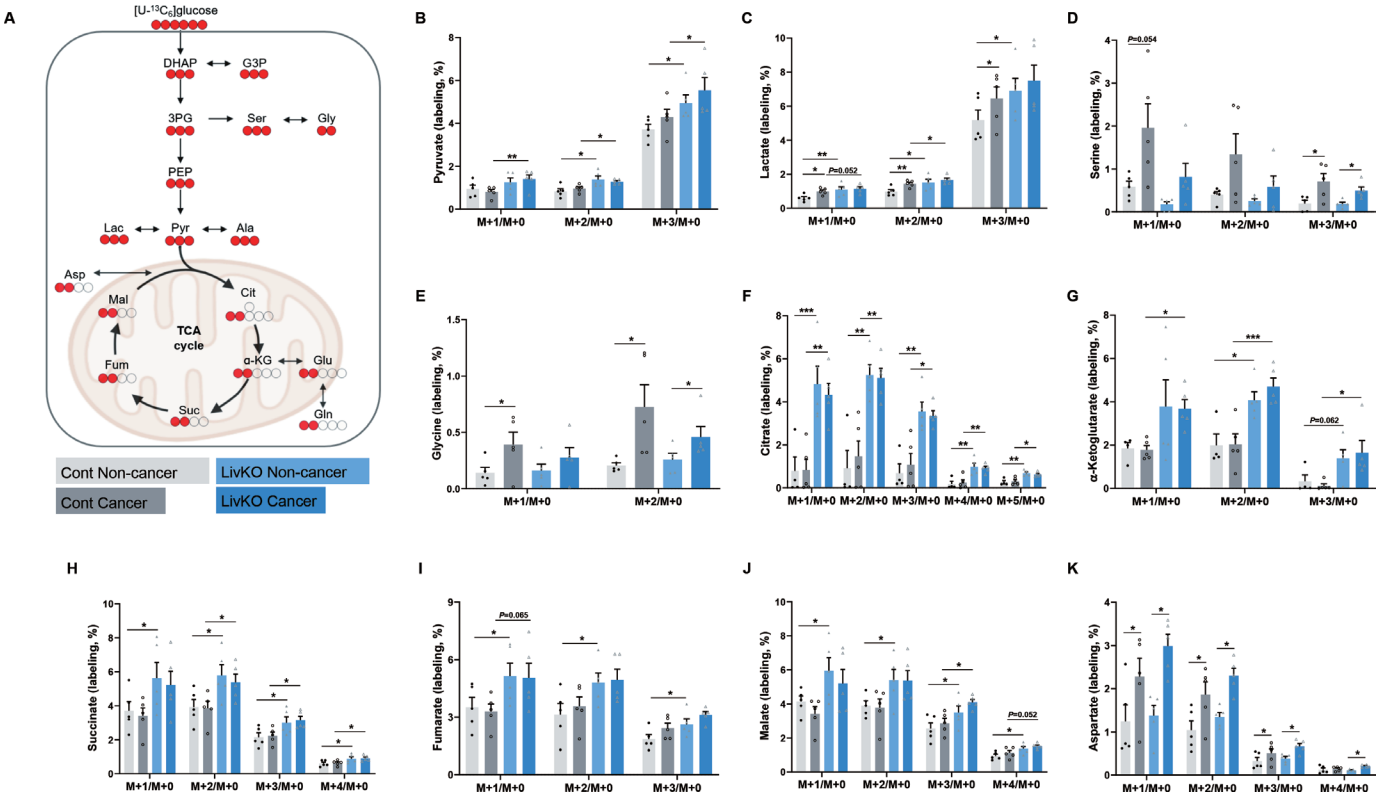

Figure 3 Mitoribosomal defects increase glucose entry into the TCA cycle, leading to increased lactate production and glucose-driven de novo biosynthesis of serine and glycine in tumor tissue. (A) Overview of glycolysis and mitochondrial TCA cycle pathways in hepatocytes. Atom tracing of glycolytic intermediates and TCA cycle metabolites of [U-$^{13}c_6$]-glucose (red). Mass isotopomer distributions were determined using GC-MS. Incorporation of ^{13}C atoms from [U-$^{13}c_6$]-labeled glucose into pyruvate (B), lactate (C), serine (D), glycine (E), citrate (F), α-ketoglutarate (G), succinate (H), fumarate (I), malate (J), and aspartate (K) is denoted as M+n, where n is the number of ^{13}C atoms. Data are expressed as the mean±SEM *p<0.05, **p<0.01, ***p<0.001 (B–K: one-way ANOVA). ANOVA, analysis of variance; GC-MS, gas chromatography-mass spectrometry; TCA, tricarboxylic acid.

online supplemental figure S16A–D). Serum levels of aspartate transaminase and alanine transaminase were also higher in LivKO mice than in control mice, again regardless of gender (figure 2L,M), although there was no significant difference in serum levels of total cholesterol or triglycerides between males or females (online supplemental figure S17A–C). DEN-treated LivKO mice exhibited significantly lower survival rates than control mice (figure 2N). Histological assessment of the liver revealed that LivKO mice developed features of chronic liver disease on DEN injection, including steatohepatitis, lobular mixed inflammation, and cellular proliferation, whereas control mice did not (online supplemental figure S17D,E).

Glucose partitioning toward glycolysis, de novo synthesis of serine and glycine, and alterations in TCA intermediates in livers with mitoribosomal defects

To assess metabolic flux directly in vivo, control and LivKO male mice with DEN-induced liver cancer received [U-$^{13}C_6$]-glucose by intraperitoneal injection at 40 weeks of age. Then, biosynthetic incorporation of glucose-derived carbon into downstream metabolites was determined using gas-chromatography mass spectrometry (figure 3A). The livers of LivKO mice contained more ^{13}C-labeled pyruvate (M+2, circled yellow; M+3, circled purple) than those of control mice (figure 3B). In addition, a mitoribosomal defect or cancer formation increased the levels of glucose-derived lactate (M+1, circled yellow; M+2, circled purple) in mouse livers (figure 3C). This suggests that high glycolytic flux toward pyruvate and lactate occurs in the liver when oxidative phosphorylation is suppressed. In addition, alanine, DHAP, 3 PG, and glucose-driven de novo biosynthesis of serine and glycine was elevated in tumor tissue (M+2, circled yellow; M+3, circled purple) and compared with that in non-cancer tissue. However, these increases were less dependent on mitoribosomal function (figure 3D,E). Glucose flux toward alanine, 3 PG, and PEP synthesis was also elevated by hepatic mitoribosomal defects and cancer formation (online supplemental figure S18A–G).

Glucose-derived pyruvate required for the TCA cycle can enter the mitochondria via the mitochondrial pyruvate carrier (MPC).[19] TCA cycle defect-mediated physiological imbalances and metabolic shifts contribute to cancer progression.[20] We found that mitoribosomal defects induced higher expression of MPC1 and MPC2

in the livers of LivKO mice than in those of control mice (online supplemental figure S19A,B). To examine whether a mitoribosomal defect-mediated increase in mitochondrial pyruvate flux induces changes in the TCA cycle, we measured the levels of [U-$^{13}C_6$]-glucose-derived hepatic TCA intermediates in LivKO mice during hepatic tumorigenesis. As shown in figure 3F–J, the levels of glucose-derived TCA intermediates were dependent on mitoribosomal function, such that the levels of ^{13}C-labeled citrate, α-ketoglutarate, succinate, fumarate, and malate (M+2, circled yellow; M+4, circled purple) were higher when a mitoribosomal defect occurred in the liver. The level of glucose-derived aspartate was higher in cancer tissue than in non-cancer tissue in control and LivKO mice (figure 3K). Taken together, these data suggest that a mitoribosomal defect induces alterations in hepatic glucose metabolism, thereby promoting glucose-derived synthesis of pyruvate and lactate and directing pyruvate toward TCA metabolism.

Knockout of *Crif1* promotes PD-1 expression by immune cells in the hepatic tumor microenvironment

In addition to metabolic alterations, we analyzed the inflammatory characteristics of tumor-bearing liver tissue in control and LivKO mice using flow cytometry (online supplemental figure S20). First, we analyzed expression of PD-1 by lymphocytes isolated from the celiac, portal, and mesenteric lymph nodes, which are the main liver draining lymph nodes for T cell priming.[21] Consistent with a previous report,[22] we found that the percentages of PD-1 +CD4+and PD-1 +CD8+T cells in the liver tumor were significantly higher than those in lymph nodes adjacent to the liver tumor (online supplemental figure S21A,B). In addition, we found higher expression of *Havcr2*, *Lag3*, and *Tox* in CD8 +T cells from tumor-bearing liver tissue than in to those from lymph nodes (online supplemental figure S21C). Next, we found that the population of natural killer (NK) T cells was lower in both male and female LivKO mice (online supplemental figure S22A); however, the percentage of NK cells and mature T cells was not different between tumor tissues from control and LivKO mice (online supplemental figure S22B–D). The relative number of tumor-infiltrating CD4 +T cells was lower in LivKO mice than in control mice (online supplemental figure S22E–G), but the number of CD8 +cytotoxic T cells was significantly higher in tumor-bearing liver tissue from LivKO mice (online supplemental figure S22E–G). The relative percentages of hepatic tumor-infiltrating neutrophils (CD11b+Ly6G+) and monocytes (CD11b+Ly6C+) were higher in LivKO mice than in the control mice (online supplemental figure S22H,I). Moreover, the population of regulatory T cells (Tregs) was significantly higher in hepatic tumor tissues from both male and female LivKO mice (online supplemental figure S22J), although CD3-B220+B cells and eosinophil numbers remained unaltered (online supplemental figure S22K–N).

Next, we investigated expression of PD-1 (also known as CD279) by tumor-infiltrating immune cells from LivKO and control mice (figure 4A–F;online supplemental figure S23A–F). Tumorous CD3 +and cytotoxic CD8 +T cells from LivKO mice showed significantly higher expression of PD-1 than those from control mice, whereas there was no significant difference in PD-1 expression between CD4 +T cells in tumor-bearing liver tissue from control and LivKO mice (figure 4A–F; online supplemental figure S23A–C). However, tumor-infiltrating CD4 +T cells from male mice exhibited a higher expression of PD-1 than those from female mice (figure 4C,D). Tumorous T cells and NKT cells showed higher expression of PD-1 than T cells and NKT cells from non-tumor tissues, regardless of *Crif1* deficiency (online supplemental figure S24A–D). Expression of *Tim3*, *Lag3*, and *Casp3* was higher in CD4 +and CD8+T cells in tumor-bearing liver tissue from LivKO mice than from control mice (online supplemental figure S25A–C). NKT cells from LivKO mice exhibited significantly higher PD-1 expression than those from the control mice (figure 4G,H; online supplemental figure S23D). Consistent with the PD-1 expression data from T cells, populations of interferon (IFN)-γ- producing CD4 +and CD8+T cells were significantly lower in DEN-treated LivKO mice, regardless of gender (figure 4I–L). However, there were no changes in the PD-1 expression by NK cells and B cells from LivKO and control mice (males or females) (figure 4M–P; online supplemental figure S23E, F). Collectively, these data suggest that tumor-infiltrating T cells from DEN-injured mice with hepatic mitoribosomal defects show a more exhausted phenotype.

Use of single-center patient data from a Korean population to assess the association between MRPs and HCC prognosis

To validate the results from the TCGA dataset, we studied expression of several MRPs in tumor tissues derived from HCC patients at CNUH. The baseline characteristics of the HCC patients are summarized in online supplemental table S2. In line with the TCGA data, the patients in our cohort with advanced-stage disease exhibited higher expression of *MRPL9*, *MRPL11*, *MRPS29*, *MPRL17*, *MRPS30*, and *CRIF1* in tumor tissue than patients with early-stage HCC (figure 5A). Based on the finding of an association between hepatic mitoribosomal dysfunction and tumorous T cell exhaustion in DEN-treated mice, we analyzed tumor-infiltrating T cells in HCC patients. Interestingly, PD-1 expression by CD4 +and CD8+T cells infiltrating HCC was significantly higher in patients with elevated MRP expression (figure 5B,C). Expression of IFN-γand Granzyme B by tumorous CD4 +and CD8+T cells from HCC patients with elevated MRP expression was reduced markedly (figure 5D,E). Moreover, expression of *IFNG* and *GZMB* was significantly lower in mononuclear cells infiltrating HCC from patients with high-MRP expression (figure 5F). By contrast, *EOMES* expression was significantly higher in tumorous mononuclear cells from patients with high-MRP expression (figure 5F). These data suggest that MRP expression is associated with cancer progression and tumorous T cell exhaustion in Korean HCC patients.

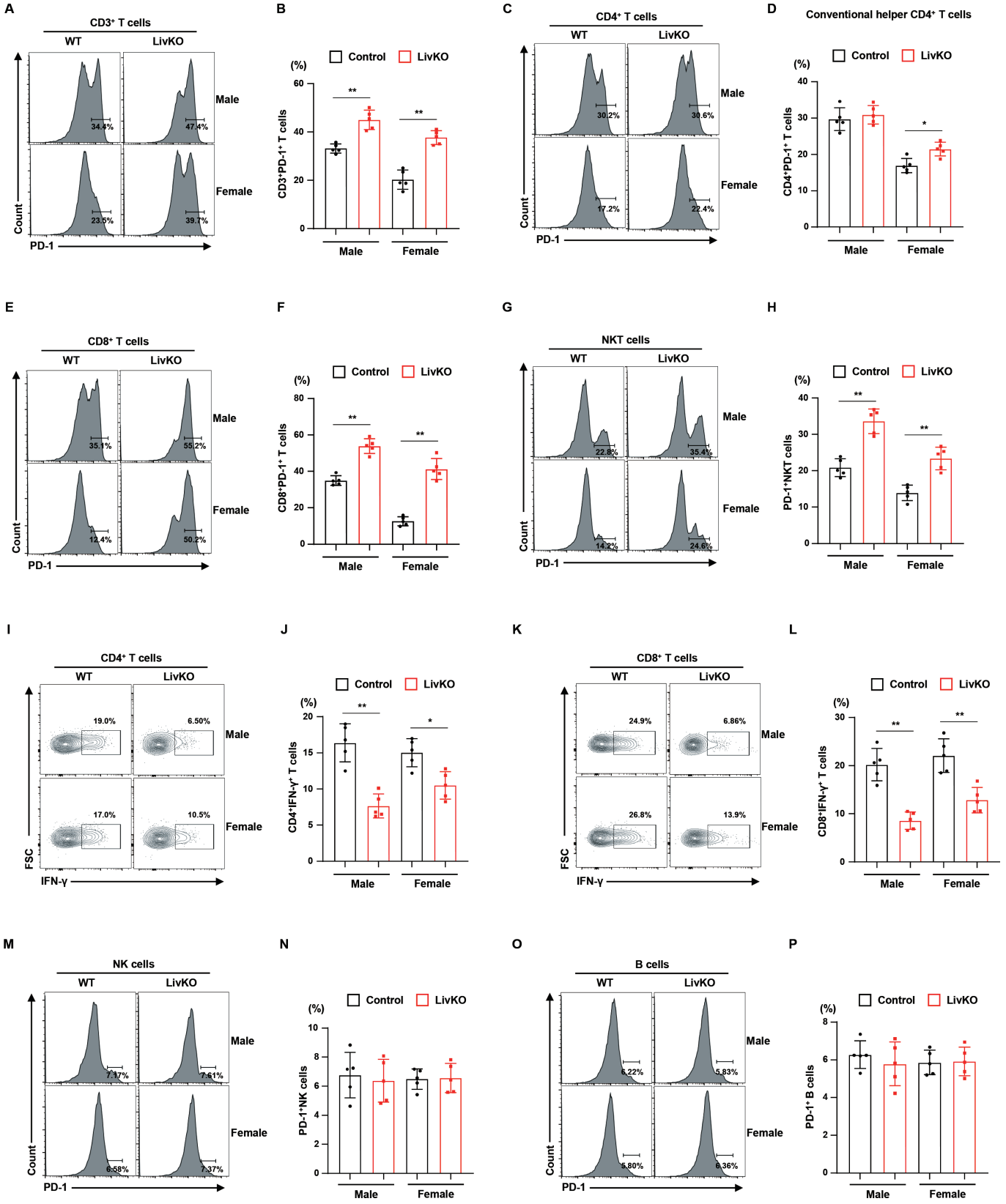

Figure 4 Hepatic mitoribosomal defects increase expression of PD-1 by tumor-infiltrating immune cells in DEN-induced liver cancer. Hepatic tumor tissues from DEN-treated control and LivKO mice (40 weeks of age) were compared. (A, B) Populations and percentages of CD3 +T cells showing high PD-1 expression. (C–F) Populations and percentages of CD4 + and CD8+T cells showing high PD-1 expression. (G, H) Populations and percentages of NKT cells showing high PD-1 expression. (I–L) Representative flow cytometry plots and percentages of IFN-γ-producing CD4 + and CD8+T cells. (M–P) Populations and percentages of NK cells and B cells showing higher PD-1 expression. Data are expressed as the mean±SEM *p<0.05, **p<0.01 (B, D, F, H, J, L, N, P: two-tailed t-tests). NK, natural killer.

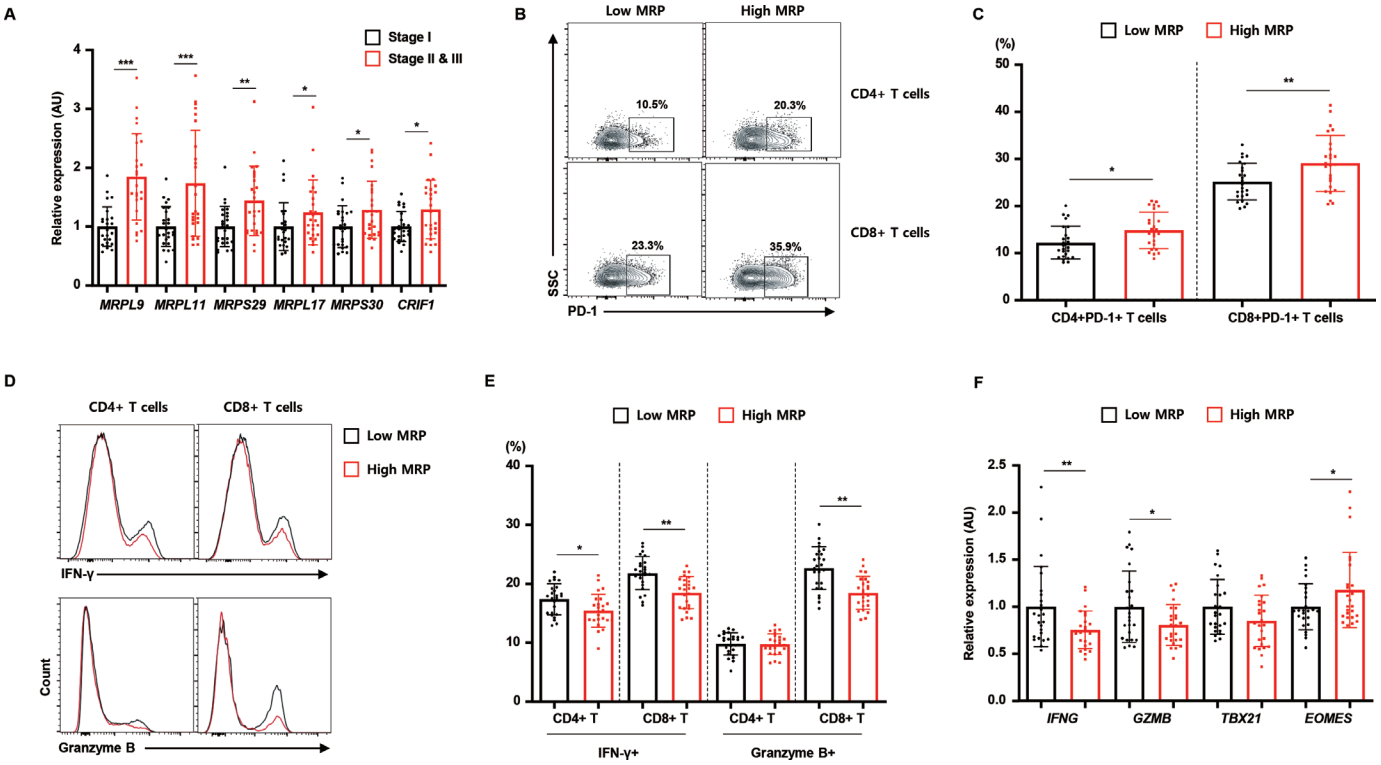

Figure 5 HCC patients with high expression of MRP exhibit an exhausted tumor-infiltrating T cell phenotype. (A) qRT-PCR analysis of MRP expression in tumor tissue from HCC patients. Tumor tissues from HCC patients were compared with respect to MRP expression. (B, C) Populations and percentages of CD4 + and CD8+T cells with high PD-1 expression. (D, E) IFN-γ production by CD4 + and CD8+T cells. (F) qRT-PCR data showing expression of *IFNG*, *GZMB*, *TBX21*, and *EOMES* by tumorous mononuclear cells from HCC patients according to tumorous MRP expression. Data are expressed as the mean±SEM *p<0.05, **p<0.01, ***p<0.001 ((A, C, E, F): two-tailed t-test). HCC, hepatocellular carcinoma; MRP, mitoribosomal protein; qRT-PCR, quantitative reverse transcription-PCR.

Hepatic mitoribosomal dysfunction causes tumor-infiltrating T cells to display a less-activated, exhausted phenotype

Metabolic reprogramming of T cells in the tumor microenvironment can lead to liver cancer progression.[23] Therefore, we measured the OCR and ECAR in CD4 + and CD8+T cells isolated from HCC tumors from control and LivKO mice. CD4 +and CD8+T cells in HCC tumor tissue from LivKO mice showed a lower ECAR than those from control mice (figure 6A,B). However, there was no difference in the OCR of tumor-infiltrating CD4 + and CD8+T cells between LivKO and control mice (figure 6C,D). We observed a significantly higher OCR/ECAR ratio in tumor-infiltrating CD4 +and CD8+T cells from LivKO mice than in those from control mice (figure 6E,F). Secretion of IFN-γ, an antitumor cytokine, was also lower in hepatic tumorous CD4 +or CD8+T cells from LivKO mice (figure 6G,H). Moreover, expression of immune function-related genes *Ifng*, *Tnf*, and *Tbet* was significantly downregulated in CD4 +and CD8+T cells from HCC tumor in LivKO mice, whereas that of *Eomes* was higher (figure 6I,J). We also confirmed that expression of anti-apoptotic proteins was downregulated significantly in tumor-infiltrating CD8 +T cells from LivKO mice (figure 6K–N). This suggests that lower glycolytic potential and exhaustion of CD4 +or CD8+T cells are associated with mitoribosomal defect-mediated progression of liver cancer.

Hepatic mitoribosomal defects induce an environment unfavorable to T cells, leading to exhaustion of T cells via elevation of ROS and lactate production

Besides suppressing antitumor immunity in LivKO mice, mitoribosomal defects may increase levels of ROS, which may contribute to liver cancer progression. HCC transcriptomic data from TCGA database revealed that expression of the ROS gene set was significantly higher in the high-MRP group than in the low-MRP group (online supplemental figure S26A). To validate this, we measured ROS levels in primary hepatocytes from control or LivKO mice via 2'–7'-dichlorofluorescin diacetate staining. Intracellular ROS levels were significantly higher in primary hepatocytes from LivKO mice than in those from control mice (online supplemental figure S26B), which might promote an environment unfavorable to T cells.[24]

Next, based on the data showing higher glycolytic flux toward lactate (figure 3C), as well as previous reports that lactate affects expression of effector cytokines such as IFN-γ and IL-2 in cultured human T cells,[25 26] we analyzed the TCGA database to investigate regulation of the lactate 'gene set' by MRP in HCC patients. Expression of the lactate gene set, including *LDHA*, was upregulated significantly in the high-MRP group compared with that in the low-MRP group (figure 7A,B). To investigate

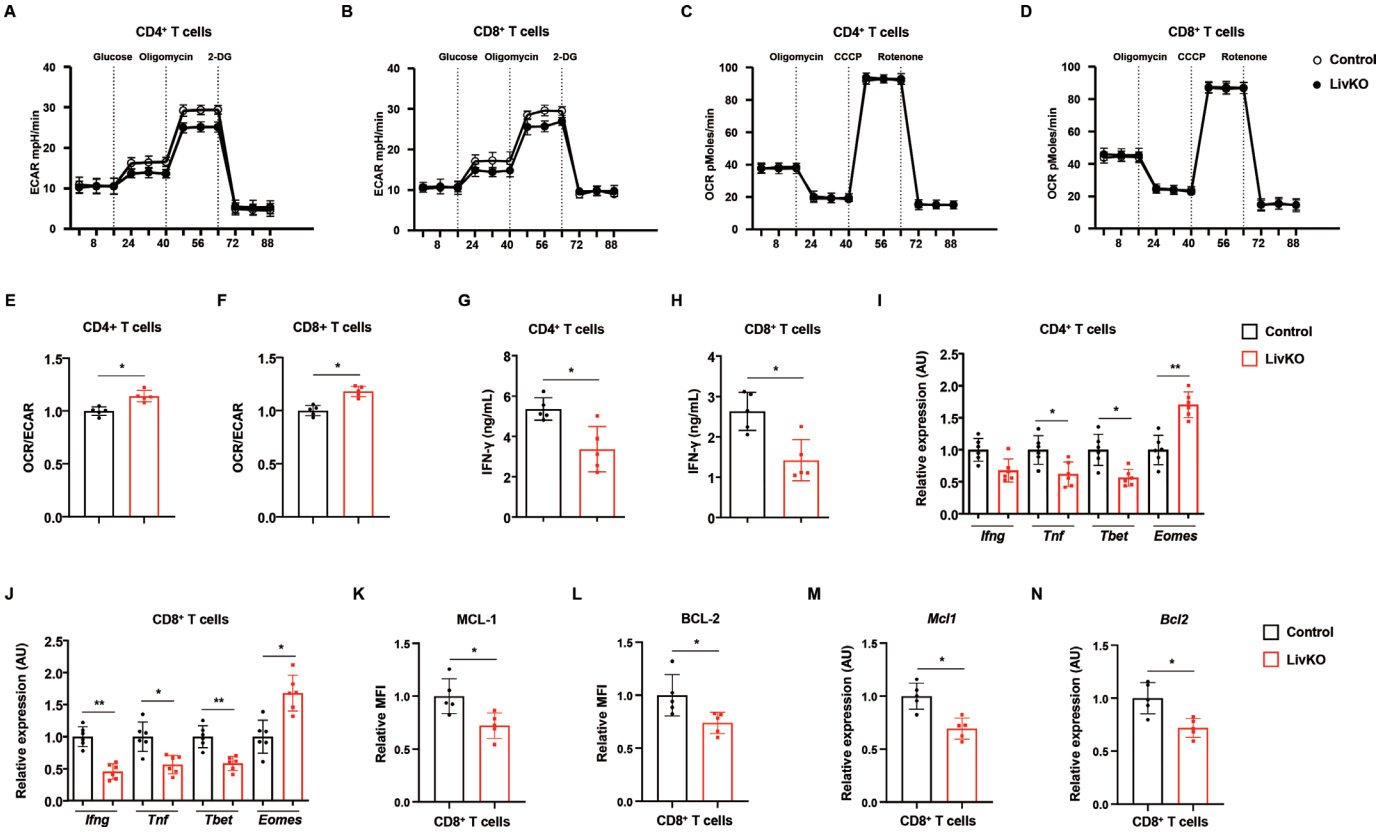

Figure 6 Hepatic mitoribosomal defects cause tumor-infiltrating CD8 +T cells to show an exhausted and apoptotic phenotype. Functional markers of cellular respiration and glycolysis expressed by tumor-infiltrating T cells from DEN-treated control and LivKO mice (40 weeks of age) were compared. (A–D) ECAR and OCR was measured in tumor-infiltrating CD4 + and CD8+T cells. (E, F) The OCR/ECAR ratio in CD4 +and CD8+T cells from liver tumors. (G, H) IFN-γ levels in the supernatant of tumor-infiltrating CD8 +T cells cultured with anti-CD3 (2 µg/mL)/CD28 (5 µg/mL) for 48 hours. (I, J) qRT-PCR analysis showing expression of *Ifng*, *Tnf*, *Tbet*, and *Eomes* mRNA in stimulated (PMA 5 ng/mL/ionomycin 500 ng/mL) tumor-infiltrating CD4 + and CD8+T cells. (K, L) Flow cytometry data showing survival markers expressed by CD8 +T cells from liver tumors. (M, N) qRT-PCR data showing expression of survival markers by CD8 +T cells from liver tumors. Data are expressed as the mean±SEM *p<0.05, **p<0.01 (E–N: two-tailed t-tests). ECAR, extracellular acidification rate; OCR, oxygen consumption rate.

the role of hepatic mitoribosomal defects on glucose-mediated plasma lactate enrichment, control and LivKO mice received a constant infusion of [U-$^{13}C_6$]-glucose via a jugular vein catheter for 150 min. Labeled plasma glucose levels were significantly higher in LivKO mice than in control mice, but the glucose turnover rate was lower, suggesting that hepatic mitoribosomal defects reduce endogenous glucose synthesis, largely reflecting suppression of hepatic glucose production (online supplemental figure S27A–D). Plasma lactate levels observed at isotopic steady state in LivKO mice were significantly higher than in control mice (figure 7C), whereas plasma lactate levels and the area under the curve at 150 min were not significantly different between control and LivKO mice (figure 7D,E). To further define the role of hepatic mitoribosomal defects on lactate levels in the context of liver cancer, we measured serum and intratumoral lactate, and found higher levels of both in DEN-treated LivKO mice than in control mice (figure 7F). We next investigated whether lactate inhibits expression of cytokines and anti-apoptotic proteins in CD8 +T cells in vitro. Mouse CD8 +T cells were stimulated in the absence or presence of different lactate concentrations, and intracellular IFN-γ and B-cell lymphoma-2 (BCL-2) levels were measured by flow cytometry. Treatment with lactate reduced expression of IFN-γ and BCL-2 (figure 7G,H). Moreover, quantitative reverse transcription-PCR showed lower expression of *Ifng* and *Mcl1* in CD8 +T cells treated with lactate in vitro (figure 7I,J). These data demonstrate that high lactate levels prevent expression of IFN-γ by CD8 +T cells in mice with hepatic mitoribosomal defects, which may be linked to promotion of immune evasion and tumor growth.

DISCUSSION

In this study, single-cell transcriptomics data analysis revealed aberrant expression of MRPs, mitochondrial stress response proteins, and hypoxia marker genes in malignant cells from HCC tumor samples. In addition, we observed that among TCGA HCC cases, aberrant expression of MRPs predicts tumor progression and prognosis. Using a mouse model with mitoribosomal defects, we also found that hepatic mitoribosomal dysfunction induced tumor growth

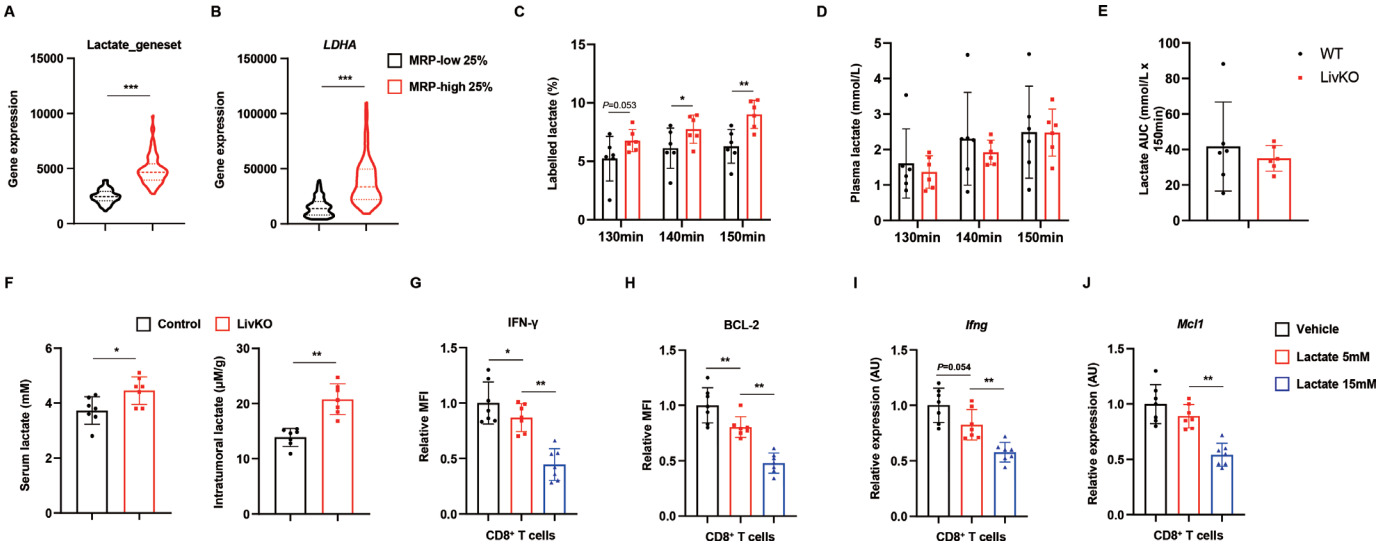

Figure 7 Lactate production induced by hepatic mitoribosomal defects increases CD8 +T cell exhaustion. (A, B) TCGA dataset analysis of HCC samples. Black and red plots represent expression of the lactate gene set and the *LDHA* gene by the lowest 25% (n=92) and highest 25% (n=92) percentiles, respectively, according to MRP expression. Labeled (C) and total (D) serum lactate levels at 130, 140, and 150 min after initiation of tracer infusion in control and LivKO mice. (E) Area under the curve (AUC) for serum lactate at 150 min. (F) Serum and intratumoral lactate concentrations in 40-week-old DEN-treated control and LivKO mice. (G, H) Flow cytometry data showing expression of IFN-γ and BCL-2, and (I, J) qRT-PCR data showing expression of *Ifng* and *Mcl1*, by CD8 +T cells from 10-week-old control mice, incubated in the absence or presence of lactate for 24 hours. Data are expressed as the mean±SEM *p<0.05, **p<0.01 (A–F: two-tailed t-tests; G–J: one-way ANOVA). ANOVA, analysis of variance; HCC, hepatocellular carcinoma; TCGA, The Cancer Genome Atlas.

and affected T cell-mediated antitumor immunity in the tumor microenvironment. In the light of mitochondrial dysfunction in HCC, expression profiles of mitoribosomal genes can be considered as critical biomarkers of disease severity and progression in HCC patients.

Considering the evidence that links mitochondria with cellular bioenergetics, generation of building blocks, and cancer progression and metastasis,[1] we hypothesized that altered mitoribosomal function might contribute to cancer progression via cellular reprogramming of nutrient acquisition and metabolism. In this study, we observed that aberrant expression of MRPs predicted overall and disease-free survival of HCC patients. In line with this, liver tumors display a general increase in MRP levels, although mitochondrial OxPhos might have limited relevance with respect to colon and renal tumors.[3 27] A plausible explanation for this is that the liver is a metabolic hub that regulates the homeostasis of carbohydrate, lipid, and protein metabolism, which is closely related to mitochondrial biology and function. Furthermore, mutations affecting MRPs are associated with liver dysfunction in humans.[28 29] Considering this evidence, we believe that mitoribosomal defects may play a crucial role in HCC progression.

Although hepatic mitoribosomal defects worsened DEN-induced liver cancer in mice, the relationship between mitochondrial stress and mitoribosomal gene expression in HCC was merely correlative, and requires further confirmation by follow-up studies. High expression of MRPs may be necessary to suppress disease progression by redressing mitochondrial proteostatic imbalances. In addition, the mitochondrial stress response is an adaptive cellular response to a diverse array of cellular stressors, including tumorigenesis. In fact, tumor cells show altered expression of a variety of mitochondria-related genes, which play a protective role in cellular adaptation to the hypoxic tumor microenvironment.[30] Moreover, MRPS5 participates in metabolic flexibility of liver cancer stem cells to facilitate tumor progression.[31] MRPS29, MRPS30, and MRPS41 induce apoptosis, which is probably mediated by Bcl2 and caspase family members.[32–34] In addition, suppression of MRPL13 or MRPS31 is a key upstream regulator of mitochondrial OxPhos dysfunction and hepatoma cell invasiveness.[35 36] Moreover, mitoribosome defects in HCC promote an aggressive phenotype via immunosuppression and immune evasion.[27] These studies suggest that suppression of MRPs-mediated bioenergetic dysfunction plays a major role in progression of liver cancer by impairing responses in tumor cells that protect against mitochondrial stress.

Recently, mitochondrial respiratory defects were linked with cancer progression via mitochondrial retrograde signaling-mediated transcriptional regulation. *CRIF1* (also known as *MRPL59*) is a component of the mitoribosomal system, and is essential for the synthesis of OxPhos polypeptides and for subsequent insertion of OxPhos subunits into the inner mitochondrial membrane.[8] Consistent with our findings, a previous study detected high expression of CRIF1 in various human HCC cell lines, as well as in primary HCC tissues.[14] Moreover, *Crif1* deficiency induces accumulation of misfolded OxPhos polypeptides in the mitochondrial matrix, which promotes the hepatic

mitochondrial unfolded protein response. This is also involved in mitochondrial respiratory defect-induced activation of the NUPR1-granulin pathway, which leads to progression of liver cancer in mice,[37] suggesting that mitochondrial ribosomal defects communicate with the nucleus through mitochondrial retrograde signaling, which contributes to cancer progression. Therefore, experimental models of *Crif1* deficiency only in tumor cells may be valuable for examining the effect of mitoribosomes on liver cancer. However, in contrast to our findings, the previous study showed that CRIF1 promoted growth and metastasis of human HCC cell lines through activation of ROS/NF-κB signaling.[14] CRIF1 expression is upregulated in osteosarcoma tissues in in vitro and xenograft models, and its translocation to the nucleus is associated with resistance of osteosarcoma cells to radiotherapy.[38] In contrast to the findings from the in vitro and xenograft models, we demonstrated that mitoribosomal defects induced by *Crif1* deficiency play a significant role in the progression of liver cancer in vivo. Tumor cells are surrounded by fibroblasts, endothelial cells, immune cells, and the extracellular matrix; this tumor microenvironment is a critical factor that determines the characteristics of each tumor and affects the growth and metastasis of cancer cells. Therefore, to overcome these limitations of the in vitro and xenograft models, we examined the role of CRIF1 in vivo using a DEN-injured liver cancer model, which has advantages as a preclinical model for studying the tumor microenvironment.

Although many kinds of mouse models show mitochondrial dysfunction, there is no available animal model harboring a mitoribosomal defect in which liver cancer experiments can be performed. However, in 2012, our group using used *Crif1* (*Mrpl59*) knockout technology to generate the first mouse model harboring mitoribosomal defects.[8] In this study, we show that CRIF1 interacts with nascent OxPhos polypeptides and molecular chaperones, and that depletion of *Crif1* leads to aberrant synthesis and defective insertion of mtDNA-encoded nascent OxPhos polypeptides into the mitochondrial inner membrane. Although expression of many MRPs, including *Mrpl59*, are changed markedly in tumor cells, we have abundant research experience using the mouse model of *Crif1* deficiency with mitoribosomal dysfunction. We chose the *Crif1* knockout mouse model to study the role of mitoribosomal function in liver cancer; however, further studies using animal models based on other MRPs are needed to elucidate the relative importance of mitoribosomal dysfunction in liver cancer.

A common feature of cancer metabolism is increased glucose uptake and glucose flux to pyruvate and lactate, as well as the use of glycolysis and TCA cycle intermediates for biosynthesis and ATP production.[39] Moreover, movement of metabolites across the mitochondrial membrane might play a crucial role in tumor growth.[40] In this study, we performed metabolic flux analysis to better understand the metabolic consequences of *Crif1* deficiency-induced mitoribosomal defects in the liver. While the principal metabolic alterations in HCC tumors are elevated glycolysis and reduced TCA cycle flux,[41] we found an increase in the levels of glycolysis-related metabolites and TCA cycle intermediates, concomitant with hepatic ribosomal defects. Furthermore, we found no significant difference in levels of ^{13}C-labeled TCA intermediates of citrate, α-ketoglutarate, fumarate, and malate between non-cancer and cancer tissues, although *Crif1* deficiency increased the amounts of ^{13}C-labeled TCA intermediates both in non-cancer and cancer tissues from the DEN-injured liver cancer model. In our previous report, a high glycolytic profile was obtained on inhibition of mitochondrial respiration by *Crif1* knockout in hepatocytes, as evidenced by a drop in OCR and a concomitant increase in ECAR.[42] Moreover, hepatic transcriptomics data revealed that *Crif1* deficiency increased expression of gene sets related to glycolysis, and induced enrichment of gene sets related to glutamine, 1C, glycogen, and fatty acid metabolism,[42] which may replenish TCA intermediates during tumor progression. These data suggest that TCA intermediates resulting from *Crif1* deficiency are used as building blocks for macromolecule synthesis, and as energy and electron acceptors that are utilized in the electron transport chain.

Moreover, specialized metabolic reprogramming of tumor cells not only induces tumor proliferation but can also inhibit generation of an effective antitumor immune response.[43 44] Our data suggest that energetics switching in tumor cells toward glycolytic metabolism induces exhaustion of tumor-infiltrating T cells. We observed a markedly higher OCR/ECAR ratio in tumor-infiltrating T cells from LivKO mice, which indicates short-lived and low-level activation. These changes in cellular metabolism and energetic reprogramming attenuate the antitumor immune response during hepatic tumorigenesis. Another important question is how are mitoribosomal defects in parenchymal cells related to exhaustion of tumor-infiltrating T cells in mice? In this study, excess lactate caused by hepatic mitoribosomal defects contributed to inhibition of antitumor responses by tumor-infiltrating T cells both in vitro and in vivo. Although this observation may provide key clinical insights into the role of lactate both in the hepatic tumor environment and in mitoribosomal defect-induced liver cancer progression, mitochondrial stress and increased lactate production by hepatocytes, as well as exhaustion of tumor-infiltrating T cells, are not sufficient to explain increased tumorigenesis in the absence of DEN-mediated hepatic injury. This means that progression of liver cancer may be driven by a defect in tumor surveillance by hepatic T cells in the DEN-injured liver. Moreover, previous investigations revealed that mitoribosomal deficiencies are associated with immunosuppression and evasion, which may be critically involved in the development of liver cancer.[27 35] However, further studies are required to uncover the precise mechanism by which mitoribosomal defects generate a protumor microenvironment and suppress antitumor immunity by increasing tumorous lactate levels during progression of liver cancer.

Lastly, the relative contribution of CD4 + and CD8+T cells to tumor regression should be investigated in the DEN-injured cancer model. First, CD8 +T cells, rather than CD4 +T or NK cells, are necessary for environmental eustress-mediated tumor repression in the DEN-injured liver cancer model.[45] Moreover, CD8 +T cells promote HCC in NASH; CD8 +PD1+T cells trigger transition to HCC in mice with NASH, probably due to impaired tumor surveillance and enhanced T cell-mediated tissue damage.[46] In addition, formation and progression of liver cancer are increased markedly in T/B cell-deficient (Rag1) mice treated with DEN.[47] These results suggest that T cells in liver tumors may become exhausted, which is a barrier to development of a robust adaptive antitumor immune response. However, further studies using T cell-depleting antibodies are required to identify the subtype of T cell that affects progression of DEN-induced liver cancer.

In conclusion, our data derived from humans studies (TCGA database and a private cohort) and a mouse model of HCC with mitoribosomal defects highlight the role of MRPs in tumorous lactate-mediated alterations of the hepatic tumor microenvironment, and subsequent progression of HCC. We also identified changes in glucose partitioning toward glycolytic flux and production of TCA cycle intermediates in livers harboring hepatic mitoribosomal defects. Finally, we suggest that immunotherapy targeting the PD-1/PD-L1 checkpoint pathway may show clinical efficacy as a treatment for specific subsets of patients with HCC; efficacy may depend on tumorous expression of MRPs or the level of mitoribosomal dysfunction.

Author affiliations
[1]Department of Core Laboratory of Translational Research, Biomedical Convergence Research Center, Chungnam National University Hospital, Daejeon, South Korea
[2]Laboratory of Endocrinology and Immune System, Chungnam National University School of Medicine, Daejeon, South Korea
[3]Department of Medical Science, Chungnam National University School of Medicine, Daejeon, South Korea
[4]Department of Surgery, Chungnam National University School of Medicine, Daejeon, South Korea
[5]National Bioinformatics Infrastructure Sweden (NBIS), Science for Life Laboratory, Stockholm, Sweden
[6]Department of Health Sciences and Technology, Gachon Advanced Institute for Health Sciences & Technology (GAIHST), Incheon, South Korea
[7]Department of Molecular Medicine, College of Medicine, Gachon University, Incheon, South Korea
[8]Department of Geriatrics, the Center for Translational Research in Aging & Longevity, Donald W. Reynolds Institute on Aging, University of Arkansas for Medical Sciences, Little Rock, AR, USA
[9]Department of Internal Medicine, Chungnam National University School of Medicine, Daejeon, South Korea
[10]School of Life Sciences, Gwangju Institute of Science and Technology, Gwangju, South Korea

Contributors H-SY designed and supervised the study, and wrote the manuscript. SL, B-SS and I-YK performed the experiments, analyzed data, and wrote the manuscript. JSM, S-HK, SGK, JTK, JWT, HTN, HYL, BCS, YK, SP and HSE performed experiments and analyzed data. SL, RB, RRW and MS critically reviewed the manuscript and provided valuable comments. H-SY is guarantor. All authors have read and approved the final manuscript.

Funding This work was supported by the Basic Science Research Program under the National Research Foundation of Korea (NRF), funded by the Ministry of Science, ICT, and Future Planning, Korea (NRF-2021R1A2C4001829). H-SY was supported by NRF (NRF-2022M3A9B6017654, NRF-2021R1A5A8029876) and the Korea Research Institute of Bioscience and Biotechnology Research Initiative Program (KGM9992211). MS was supported by the NRF (NRF-2017R1E1A1A01075126) and by a grant from the Korea Health Technology R&D Project through the Korea Health Industry Development Institute, funded by the Ministry of Health & Welfare, Republic of Korea (grant number: HR20C0025). I-YK was supported by NRF (MSIT-2021R1A2C3005801) and by a Korea Research Fellowship, funded by the Ministry of Science and ICT and NRF (2019H1D3A1A01071043). SL was supported by 'GIST Research Institute IIBR' grants funded by the GIST in 2021, by the Bio-Synergy Research Project (2021M3A9C4000991), the Bio & Medical Technology Development Program (2021M3A9G8022959), and by an NRF grant (NRF-2021R1C1C1006336) from the Ministry of Science and ICT through the National Research Foundation.

Competing interests None declared.

Patient consent for publication Consent obtained directly from patient(s)

Ethics approval The animal study was reviewed and approved by Chungnam National University Hospital (CNUH-020-P0087). This study and protocols for human subjects were approved by the Institutional Review Board of Chungnam National University Hospital (CNUH 2015-04-014). All experiments were approved by the Institutional Review Board of CNUH. All animals received humane care according to institutional guidelines, and all experiments were approved by the Institutional Review Board of CNUH. All experimental procedures were conducted in accordance with the guidelines of the Institutional Animal Care and Use Committee of Chungnam National University School of Medicine (CNUH-019-A0071, Daejeon, Korea).

Provenance and peer review Not commissioned; externally peer reviewed.

Data availability statement Data are available in a public, open access repository. Data are available on reasonable request.

ORCID iD
Hyon-Seung Yi http://orcid.org/0000-0002-3767-1954

REFERENCES

1 Vyas S, Zaganjor E, Haigis MC. Mitochondria and cancer. *Cell* 2016;166:555–66.
2 Pearce SF, Rebelo-Guiomar P, D'Souza AR, *et al*. Regulation of mammalian mitochondrial gene expression: recent advances. *Trends Biochem Sci* 2017;42:625–39.
3 Kim H-J, Maiti P, Barrientos A. Mitochondrial ribosomes in cancer. *Semin Cancer Biol* 2017;47:67–81.
4 Amunts A, Brown A, Toots J, *et al*. Ribosome. The structure of the human mitochondrial ribosome. *Science* 2015;348:95–8.
5 HS Y, Jeong WI. Interaction of hepatic stellate cells with diverse types of immune cells: foe or friend? *J Gastroenterol Hepatol* 2013;28:99–104.
6 Robinson MW, Harmon C, O'Farrelly C. Liver immunology and its role in inflammation and homeostasis. *Cell Mol Immunol* 2016;13:267–76.
7 Ringelhan M, Pfister D, O'Connor T, *et al*. The immunology of hepatocellular carcinoma. *Nat Immunol* 2018;19:222–32.
8 Kim SJ, Kwon M-chul, Ryu MJ, *et al*. CRIF1 is essential for the synthesis and insertion of oxidative phosphorylation polypeptides

in the mammalian mitochondrial membrane. *Cell Metab* 2012;16:274–83.
9 Kramer G, Rauch T, Rist W, *et al*. L23 protein functions as a chaperone docking site on the ribosome. *Nature* 2002;419:171–4.
10 Sharma MR, Koc EC, Datta PP, *et al*. Structure of the mammalian mitochondrial ribosome reveals an expanded functional role for its component proteins. *Cell* 2003;115:97–108.
11 Baslan T, Hicks J. Unravelling biology and shifting paradigms in cancer with single-cell sequencing. *Nat Rev Cancer* 2017;17:557–69.
12 Dang CV. Links between metabolism and cancer. *Genes Dev* 2012;26:877–90.
13 Ma L, Wang L, Khatib SA, *et al*. Single-cell atlas of tumor cell evolution in response to therapy in hepatocellular carcinoma and intrahepatic cholangiocarcinoma. *J Hepatol* 2021;75:1397–408.
14 Chang H, Li J, Qu K, *et al*. CRIF1 overexpression facilitates tumor growth and metastasis through inducing ROS/NFκB pathway in hepatocellular carcinoma. *Cell Death Dis* 2020;11:332.
15 Mardinoglu A, Shoaie S, Bergentall M, *et al*. The gut microbiota modulates host amino acid and glutathione metabolism in mice. *Mol Syst Biol* 2015;11:834.
16 Patil KR, Nielsen J. Uncovering transcriptional regulation of metabolism by using metabolic network topology. *Proc Natl Acad Sci U S A* 2005;102:2685–9.
17 Kenny TC, Craig AJ, Villanueva A, *et al*. Mitohormesis primes tumor invasion and metastasis. *Cell Rep* 2019;27:2292–303.
18 Kenny TC, Gomez ML, Germain D. Mitohormesis, UPR^{mt}, and the complexity of mitochondrial DNA landscapes in cancer. *Cancer Res* 2019;79:6057–66.
19 Bricker DK, Taylor EB, Schell JC, *et al*. A mitochondrial pyruvate carrier required for pyruvate uptake in yeast, Drosophila, and humans. *Science* 2012;337:96–100.
20 Martínez-Reyes I, Chandel NS. Mitochondrial TCA cycle metabolites control physiology and disease. *Nat Commun* 2020;11:102.
21 Barbier L, Tay SS, McGuffog C, *et al*. Two lymph nodes draining the mouse liver are the preferential site of DC migration and T cell activation. *J Hepatol* 2012;57:352–8.
22 Zheng M, Yu J, Tian Z. Characterization of the liver-draining lymph nodes in mice and their role in mounting regional immunity to HBV. *Cell Mol Immunol* 2013;10:143–50.
23 Ma L, Hernandez MO, Zhao Y, *et al*. Tumor cell biodiversity drives microenvironmental reprogramming in liver cancer. *Cancer Cell* 2019;36:418–30.
24 Zhang Z, Liu S, Zhang B, *et al*. T cell dysfunction and exhaustion in cancer. *Front Cell Dev Biol* 2020;8:17.
25 Brand A, Singer K, Koehl GE, *et al*. LDHA-Associated lactic acid production blunts tumor immunosurveillance by T and NK cells. *Cell Metab* 2016;24:657–71.
26 Fischer K, Hoffmann P, Voelkl S, *et al*. Inhibitory effect of tumor cell-derived lactic acid on human T cells. *Blood* 2007;109:3812–9.
27 Kwon SM, Lee Y-K, Min S, *et al*. Mitoribosome defect in hepatocellular carcinoma promotes an aggressive phenotype with suppressed immune reaction. *iScience* 2020;23:101247.
28 Lake NJ, Webb BD, Stroud DA, *et al*. Biallelic mutations in MRPS34 lead to instability of the small mitoribosomal subunit and Leigh syndrome. *Am J Hum Genet* 2018;102:713.
29 Menezes MJ, Guo Y, Zhang J, *et al*. Mutation in mitochondrial ribosomal protein S7 (MRPS7) causes congenital sensorineural deafness, progressive hepatic and renal failure and lactic acidemia. *Hum Mol Genet* 2015;24:2297–307.
30 Li X, Wang M, Li S, *et al*. HIF-1-induced mitochondrial ribosome protein L52: a mechanism for breast cancer cellular adaptation and metastatic initiation in response to hypoxia. *Theranostics* 2021;11:7337–59.
31 Wei Z, Jia J, Heng G, *et al*. Sirtuin-1/Mitochondrial ribosomal protein S5 axis enhances the metabolic flexibility of liver cancer stem cells. *Hepatology* 2019;70:1197–213.
32 Carim L, Sumoy L, Nadal M, *et al*. Cloning, expression, and mapping of PDCD9, the human homolog of Gallus gallus pro-apoptotic protein p52. *Cytogenet Cell Genet* 1999;87:85–8.
33 Chintharlapalli SR, Jasti M, Malladi S, *et al*. BMRP is a Bcl-2 binding protein that induces apoptosis. *J Cell Biochem* 2005;94:611–26.
34 Levy-Strumpf N, Kimchi A. Death associated proteins (DAPs): from gene identification to the analysis of their apoptotic and tumor suppressive functions. *Oncogene* 1998;17:3331–40.
35 Lee Y-K, Lim JJ, Jeoun U-W, *et al*. Lactate-mediated mitoribosomal defects impair mitochondrial oxidative phosphorylation and promote hepatoma cell invasiveness. *J Biol Chem* 2017;292:20208–17.
36 Min S, Lee Y-K, Hong J, *et al*. MRPS31 loss is a key driver of mitochondrial deregulation and hepatocellular carcinoma aggressiveness. *Cell Death Dis* 2021;12:1076.
37 Lee Y-K, Jee BA, Kwon SM, *et al*. Identification of a mitochondrial defect gene signature reveals NUPR1 as a key regulator of liver cancer progression. *Hepatology* 2015;62:1174–89.
38 Ran Q, Jin F, Xiang Y, *et al*. CRIF1 as a potential target to improve the radiosensitivity of osteosarcoma. *Proc Natl Acad Sci U S A* 2019;116:20511–6.
39 Pavlova NN, Thompson CB. The emerging hallmarks of cancer metabolism. *Cell Metab* 2016;23:27–47.
40 Todisco S, Convertini P, Iacobazzi V, *et al*. TCA cycle rewiring as emerging metabolic signature of hepatocellular carcinoma. *Cancers* 2019;12:12010068. doi:10.3390/cancers12010068
41 Huang Q, Tan Y, Yin P, *et al*. Metabolic characterization of hepatocellular carcinoma using nontargeted tissue metabolomics. *Cancer Res* 2013;73:4992–5002.
42 Kang SG, Choi MJ, Jung S-B, *et al*. Differential roles of GDF15 and FGF21 in systemic metabolic adaptation to the mitochondrial integrated stress response. *iScience* 2021;24:102181.
43 Chang C-H, Qiu J, O'Sullivan D, *et al*. Metabolic competition in the tumor microenvironment is a driver of cancer progression. *Cell* 2015;162:1229–41.
44 Zhao E, Maj T, Kryczek I, *et al*. Cancer mediates effector T cell dysfunction by targeting microRNAs and EZH2 via glycolysis restriction. *Nat Immunol* 2016;17:95–103.
45 Liu C, Yang Y, Chen C, *et al*. Environmental eustress modulates β-ARs/CCL2 axis to induce anti-tumor immunity and sensitize immunotherapy against liver cancer in mice. *Nat Commun* 2021;12:5725.
46 Pfister D, Núñez NG, Pinyol R, *et al*. NASH limits anti-tumour surveillance in immunotherapy-treated HCC. *Nature* 2021;592:450–6.
47 Schneider C, Teufel A, Yevsa T, *et al*. Adaptive immunity suppresses formation and progression of diethylnitrosamine-induced liver cancer. *Gut* 2012;61:1733–43.